Desalination and Water Treatment
www.deswater.com

doi: 10.5004/dwt.2021.26489

209 (2021) 24–36
January

Tuning the RO membranes using the spin-assisted layer by layer assembly of polyelectrolytes

Saqib Javed[a,b], Isam H. Aljundi[a,*]

[a]*Chemical Engineering Department, King Fahd University of Petroleum and Minerals (KFUPM), Dhahran 31261, Saudi Arabia, Tel. +966-13-860-2219; Fax: +966-13-860-4234; email: aljundi@kfupm.edu.sa (I.H. Aljundi)*
[b]*Department of Chemical, Polymer and Composite Materials Engineering, University of Engineering and Technology Lahore (KSK Campus), Pakistan*

Received 1 April 2020; Accepted 20 August 2020

ABSTRACT

Polyelectrolyte multilayer films are currently used to modify the permeation and rejection properties of thin-film composite membranes (TFC). In this paper, response surface methodology was used to study the effect and synergies between interactive parameters essential for modification of the TFC membrane. TFC membranes were prepared using *m*-phenylenediamine and trimesoyl chloride and modified by spin-assisted layer-by-layer (LbL) technique using polyethyleneimine (PEI) and polyallylamine hydrochloride as the deposition polyelectrolytes. The Box–Behnken design of experiment (DOE) was applied to investigate the effect of preparation conditions (number of deposited layers, pH, the concentration of the polyelectrolyte solutions) on the performance of the modified reverse osmosis (RO) membranes. It was found that under saline feed conditions, higher permeate flux favors higher pH and higher PEI concentration, while salt rejection favors a similar concentration of both polyelectrolytes. In addition, the PEI concentration was found to have a stronger effect on the permeate flux than that of the number of bilayers since it enhanced the hydrophilic functional groups on the membrane surface. Analysis of variance results indicated that the developed models adequately represent the relationship between the studied variables. Optimization of the preparation conditions revealed that both polyelectrolytes must be used at their maximum concentration at a pH of 7.8 with 50 bilayers of the coating. The confirmation run showed a close correlation between the prediction using the DOE and the actual experimental data. This study demonstrated the potential application of DOE to the optimization of LbL RO membrane preparation conditions.

Keywords: Desalination; RO membrane modification; Polyelectrolytes; LbL; Response surface methodology

1. Introduction

Approximately 0.8% of all water available on earth is considered to be fresh groundwater and it is not sufficient to fulfill the needs of safe drinking water [1]. The lack of clean drinking water is becoming an alarming condition all around the world [2]. According to the World Health Organization, more than 1.1 billion people did not have access to drinking water facilities [3].

The best solution to overcome water scarcity is desalination [4,5] which can be divided into two leading categories; thermal or membrane processes. Thermal desalination consumes heat and provides freshwater in the form of distillate. 50% of the world's desalination capacity is present in the Middle East and mostly uses the thermal multi-stage flash (MSF) technology [6].

However, reverse osmosis (RO) requires lower energy (2–3 kWh/m^3) for seawater desalination [7] compared to the

* Corresponding author.

high demand of 15.5 kWh/m^3 for MSF. This explains why at present, desalination plants outside the Middle East are mainly based on RO technology. By the end of 2014, the market value for RO equipment and membranes was around $5.4 billion [8]. However, the demand for major components of RO water treatment systems is expected to grow from $11.7 billion in 2020 to $19.1 billion by 2025 [9]. The drive behind this expansion is that the consumption of energy has been reduced significantly during the last few years for the RO processes along with the development of new and effective membranes [10].

Thin-film composite (TFC)-RO membranes are asymmetric multilayer films in which the common active polyamide layer is synthesized by interfacial polymerization. The preparation conditions of the membranes greatly affect their structure and eventually their performance in terms of flux and salt rejection. The properties and performance of the TFC membrane can be enhanced by several methods including the layer-by-layer (LbL) assembly of polyelectrolytes. It is a commonly used technique for surface modification due to its simplicity, robustness, and control over the membrane thickness. Many researchers have utilized the LbL for membrane modification to get improved performance [11–14].

Malaisamy et al. [11] modified the polyamide membrane by using poly(diallyl-dimethylammonium chloride) and poly(styrene sulfonate) (PDADMAC/PSS) pair of polyelectrolytes and noticed that the permeate flux decreased from around 42 to 21 L/m^2 h when the number of layers increased from 4 to 8. On the other hand, the permeate flux of the modified membrane was still 30% higher than that of the commercial BW30 RO membrane. The loss in permeate flux was solely due to the increase in the thickness of the membrane. Sulfate ions were completely rejected but the rejection of fluoride ions through the unmodified membrane was 50%, which increased considerably to 70% by coating 8 bilayers. The difference in salt rejection between these ions is due to their difference in hydration energies which is highest for sulfate ions.

Park et al. [12] used the LbL assembly of poly(allylamine hydrochloride) and poly(acrylic acid) for the coating of negatively charge polysulfone substrate. The desalination performance of the coated membranes was investigated at 20 bars with 2,000 ppm NaCl feed solution. The membrane with 20 polyelectrolyte multilayers achieved a permeate flux and salt rejection of 7 L/m^2 h and 81%, respectively. Although the polyelectrolyte membranes provided good salt rejection, the permeate flux was low.

Wang et al. [13] studied the behavior of polyamide RO membrane by depositing poly(ethylene glycol) acrylate multilayers. Permeation tests were performed using artificial seawater with 30.83 g/L NaCl and 1.11 g/L $CaCl_2$ under 55 bar. They achieved a rejection of up to 94% by depositing one and two bilayers. The increased salt rejection was relatively small which indicates a thin coating. The hurdle in achieving 99% rejection as expected in commercial RO membranes was due to higher concentration polarization in the arrangement of dead-end cell apparatus.

Ishigami et al. [14] deposited PSS/polyallylamine hydrochloride (PAH) on the commercial RO membrane and tested it under NaCl concentration of 500 mg/L. With 6 layers, the obtained permeate flux was around 3.1 L/m^2 h atm which decreased to 2.5 L/m^2 h atm by coating 12 bilayers. This was due to an increase in hydrodynamic resistance in the polyelectrolyte multi-layered RO membrane. The salt rejection, however, was improved from 98% to 99.4%.

The effect of various LbL key parameters on the performance of the membranes is discussed in detail in a comprehensive review [15]. However, the synergistic effect of multiple parameters on the performance of the RO membrane is limited in the literature. To study the effect of multiple factors simultaneously on the performance of the membranes, the design of experiment is necessary to reduce the number of required experiments and to end up with a statistical conclusion that describes the effect of multiple factors.

Response surface methodology (RSM) consists of designs and models that can deal with a response at a continuous scale and the objective implicates to find the optima. Then, the objective is accomplished by developing a statistically designed sequence of experiments. Therefore, RSM is considered as a handy tool for modeling and analysis of problems to evaluate the individual and interactive relationship between factors and responses. In this study, RSM is selected to investigate the synergistic effect of multiple preparation conditions on membrane performance and to determine the optimum conditions [16]. Box–Behnken design is a second-order design consisting of a collection of mathematical and statistical techniques that are useful for the modeling and analysis of problems. In Box–Behnken design, a response of interest is influenced by many input process variables and then objective involves optimizing that response. This optimization route starts with problem identification, determining the range of process parameters, then set of statistically designed experiments are performed followed by the data analysis [17]. The analysis of variance (ANOVA), associated with the data analysis, is a systematic way to figure out and study the significant variables affecting the response that is to be optimized [18].

Khayet et al. [19] used a RSM to develop predictive models for the optimization of operating conditions for the reverse osmosis desalination process. The polyamide TFC membranes were tested in the presence of model solutions of NaCl at brackish (6 g/L) and seawater (30 g/L) concentrations. ANOVA test showed that feed salt concentration and the operating pressure was found to be a significant parameter on the RO performance index (salt rejection times permeate flux) whereas the influence of feed flow rate was found to be negligible. Optimum operating conditions yielded 99.98% salt rejection at an optimum pressure of 13.5 bar.

Razali et al. [20] investigated the interaction and optimization of the operating variables to improve the structure and performance of polyethersulfone membranes using the central composite design of the response surface method. A strong interaction was found among the input variables including, polyaniline nanoparticles concentration and evaporation time during the casting process. Regression analysis generated the optimal point and experimental results showed only a 6% deviation from the optimum point.

To the best of our knowledge, no paper was found in the literature that used the design of the experiment to relate

the LbL preparation conditions with the performance of the membrane. Most of the previous work investigated factors one at a time and neglected the synergetic effect of those parameters or the effect of interacting parameters. Lack of models that can describe the effect of multiple LbL factors on the performance of the membranes was also a motivation for this work. Therefore, the objective of this paper is to systematically study the LbL modification of RO membranes using the design of the experiment. The combined effects of preparation conditions (number of bilayers, concentration, and pH of the polyelectrolyte solutions) on the performance of the membrane will be investigated and modeled using the RSM.

2. Experimental setup

2.1. Materials

All chemicals were purchased from Sigma-Aldrich (USA). Polysulfone (PS) pellets with a molecular weight of 35 kDa were used for the preparation of PS support. Dimethylacetamide was used as a solvent for the preparation of PS support over non-woven polyester fabric (Novatexx 2413, Freudenberg Filtration Technologies, Germany). *m*-phenylenediamine (>99%) and trimesoyl chloride (>98%) were used for the preparation of the polyamide membrane. Polyethyleneimine (PEI) with a molecular weight of 25,000 g/mol (<1% water) and PAH with a molecular weight of 120,000–180,000 g/mol was used for LbL coating. Sodium chloride (>99.5%) was used to prepare the brackish water during membrane testing.

2.2. Fabrication and modification of the polyamide RO membrane

The TFC RO membrane was fabricated on top of PS support. The support was prepared through the phase inversion process and the polyamide membrane was prepared through interfacial polymerization. Moreover, the polyamide RO membrane was modified using PEI/PAH pair of polyelectrolytes via a spin-assisted LbL technique. The membrane fabrication and its modification procedure are explicitly described in our previous publication [21].

2.3. Experimental design

The software Design-Expert 7.0 (State-Ease Inc., USA) was used for scheduling and optimization of the experiments with the Box–Behnken design. ANOVA test was performed to find the significant factors/interactions using the probability *p*-value. The suitability of the model was expressed by the coefficient of determination (R^2), adequate precision, and *F*-test.

In this study, four independent factors were selected including the number of layers, pH, the concentration of PEI, and the concentration of PAH. Pure water flux, saline water flux, and salt rejection (%) were studied as responses. The input factors with their coded and actual values are given in Table 1. The design layout of 29 experiments to study the LbL-modified membranes based on the Box–Behnken model is shown in Table 2.

A second-order model was selected to describe the responses as a function of the coded factors:

$$Y_i = b_0 + \sum_{i=1}^{n} b_i x_i + \sum_{i=1}^{n} b_{ii} x_i^2 + \sum_{i=1}^{n-1} \sum_{j=i+1}^{n} b_{ij} x_i x_j \quad (1)$$

In this equation, Y_i is the predicted response (pure water flux, saline water flux, rejection), b_0 is the intercept term, linear and second-order polynomial coefficients are represented by b_i and b_{ii} respectively. Interaction terms are given by b_{ij} whereas x_i and x_j are the coded independent variables. The relationship between the coded factors and the actual values are given by the following equations:

$$X_1 = \frac{A - 27.5}{22.5} \quad (2)$$

$$X_2 = \frac{B - 6}{2} \quad (3)$$

$$X_3 = \frac{C - 110}{90} \quad (4)$$

$$X_4 = \frac{D - 110}{90} \quad (5)$$

2.4. Desalination experiments

The filtration experiments were conducted in a cross-flow apparatus using Sterlitech CF-042 membrane cell (USA) as shown in Fig. S1 with an effective membrane area of 42 cm^2. Fig. 1 shows a schematic diagram of the test unit

Table 1
Independent factors with actual and coded levels

Independent factor	Symbol		Coded values		
	Actual	Coded	–1	0	+1
			Actual values		
Number of layers	*A*	X_1	5	27.5	50
pH	*B*	X_2	4	6	8
Polyethyleneimine, (mg/L)	*C*	X_3	20	110	200
Poly(allylamine hydrochloride), (mg/L)	*D*	X_4	20	110	200

Table 2
Experimental design layout by design expert

Run	X_1	X_2	X_3	X_4
1	27.5	8	20	110
2	50	6	110	200
3	27.5	6	110	110
4	5	6	200	110
5	5	6	20	110
6	50	6	110	20
7	27.5	6	110	110
8	27.5	8	110	200
9	5	8	110	110
10	27.5	4	200	110
11	27.5	4	110	20
12	50	8	110	110
13	27.5	4	110	200
14	27.5	6	200	200
15	27.5	8	200	110
16	50	6	20	110
17	5	6	110	20
18	27.5	8	110	20
19	50	4	110	110
20	27.5	6	200	20
21	27.5	6	110	110
22	50	6	200	110
23	27.5	6	110	110
24	5	4	110	110
25	5	6	110	200
26	27.5	6	20	200
27	27.5	4	20	110
28	27.5	6	20	20
29	27.5	6	110	110

which consists of a feed tank, pump, bypass and feed control valves, membrane assembly, and pressure gauges.

The filtration experiments were performed at a temperature of 23°C ± 2°C which was controlled using a chiller (Proline RP 1845, Lauda, Germany). Permeate flux was recorded for 2 h of continuous operation at 15 bar. The permeate flux was calculated using the following relation:

$$J_0 = \frac{V}{A \cdot t} \tag{6}$$

where J_0 is the volumetric flux (L/m² h), A is the active membrane area (m²), t is the permeation time (h), V is the permeate volume (L).

The apparent NaCl rejection was calculated by the following relation:

$$R_{\text{NaCl}} = \left(1 - \frac{C_p}{C_f}\right) \times 100 \tag{7}$$

where R_{NaCl} is the salt rejection (%), C_p is the feed salt concentration (mg/L); C_f is the concentrations of salt in the permeate (mg/L).

3. Results and discussion

The surface and cross-sectional morphologies of the membranes were studied by TESCAN field-emission scanning electron microscopy (Model JSM6400, Czech Republic). The typical ridge and valley structure of the polyamide RO membranes can be seen in Fig. 2a. The surface morphology is rough and non-uniform which is the result of interfacial polymerization [21–23]. It occurs due to the fast and uncontrolled reaction at the interface during the process of polymerization [24]. The active barrier layer is present on the membrane surface in an irregular manner. However, after the deposition of the polyelectrolyte solution on the membrane surface, an obvious disparity in surface morphology is observed as shown in Fig. 2c. With only 5 bilayers, the surface becomes fairly smooth compared to the un-modified RO membrane. The polyelectrolyte solutions penetrated the rough, ridge and valley parts of the membrane that caused the smoothness of the membrane surface. This feature is even more noticeable in the case of 27.5 and 50 bilayers as shown in Figs. 2c and d; respectively. By increasing the number of coating layers, an increase in smoothness is observed as indicated by the root mean square roughness (R_{ms}) in Table 3 [21]. More coating layers mean more deposition of polyelectrolytes solutions. The addition of the solution in the ridge and valley structure of the membrane surface will minimize the risk of deposition of foulants. Reducing the foulants will improve the performance of the modified membranes in terms of permeate flux and salt rejection [14].

The instability of physisorbed polyelectrolyte films is a major drawback for modified membranes. This instability is due to changes that may occur either to the operating conditions (T, P, Reynolds number,…), feed properties (composition, ionic strength, pH,…), surface charge, or even displacement of the polyelectrolyte polymer by adsorption of a competing compound [25,26]. However, weak attachment of the polyelectrolyte to the membrane surface (and later detachment from the surface) might be useful in applications was fouling of the membrane is a concern since the polyelectrolyte layer will be used as a protective layer for the membrane and will be washed away along with the fouling materials after some time from the start of the operation [27].

The successful deposition of the polyamide barrier layer is visible in the cross-section image as shown in Fig. 2b. The rough polyamide structure is in agreement with the findings of Jeong et al. [28] and the estimated thickness of the active layer (265 nm) is comparable with that reported by Pacheco et al. [29]. The effect of bilayer deposition is demonstrated in Figs. 2d, f, and h. By increasing the number of layers, the thickness of the barrier layer increased as shown in Table 3. The deposition of 50 polyelectrolyte multilayers developed a membrane of approximately twice the thickness of that coated by 5 bilayers. However, the thickness was lower than that reported by Seo et al. [30] using the LbL assembly of poly(ethylene oxide) and poly(acrylic acid) (PEO/PAA). An increase in the active-layer thickness

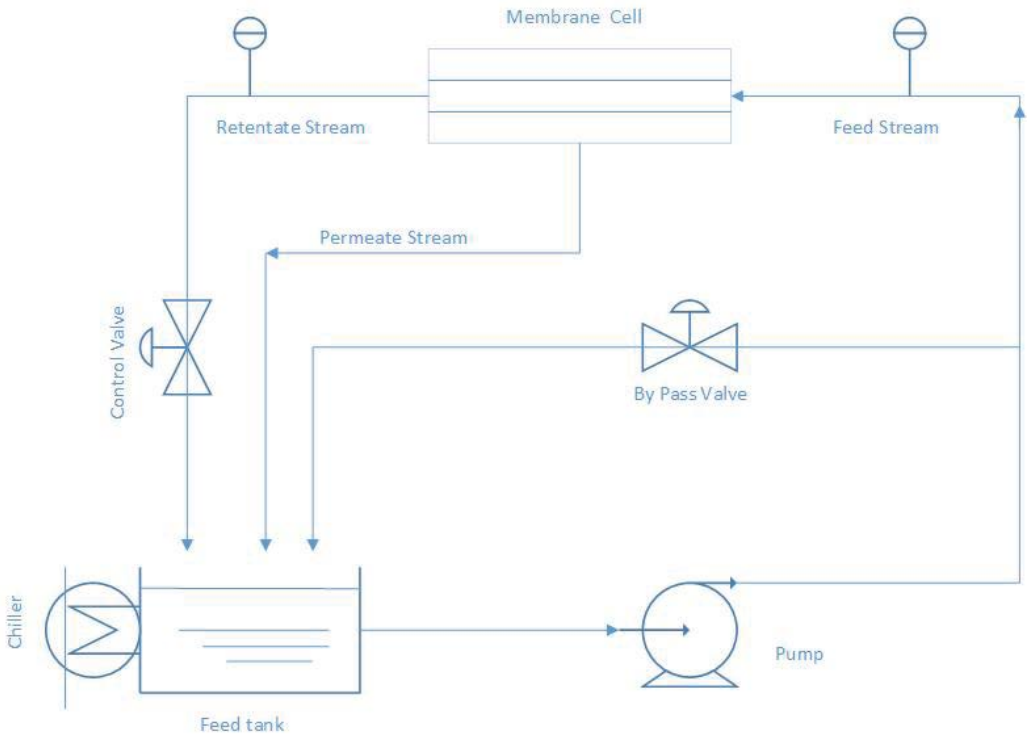

Fig. 1. Schematic diagram of the cross-flow filtration apparatus.

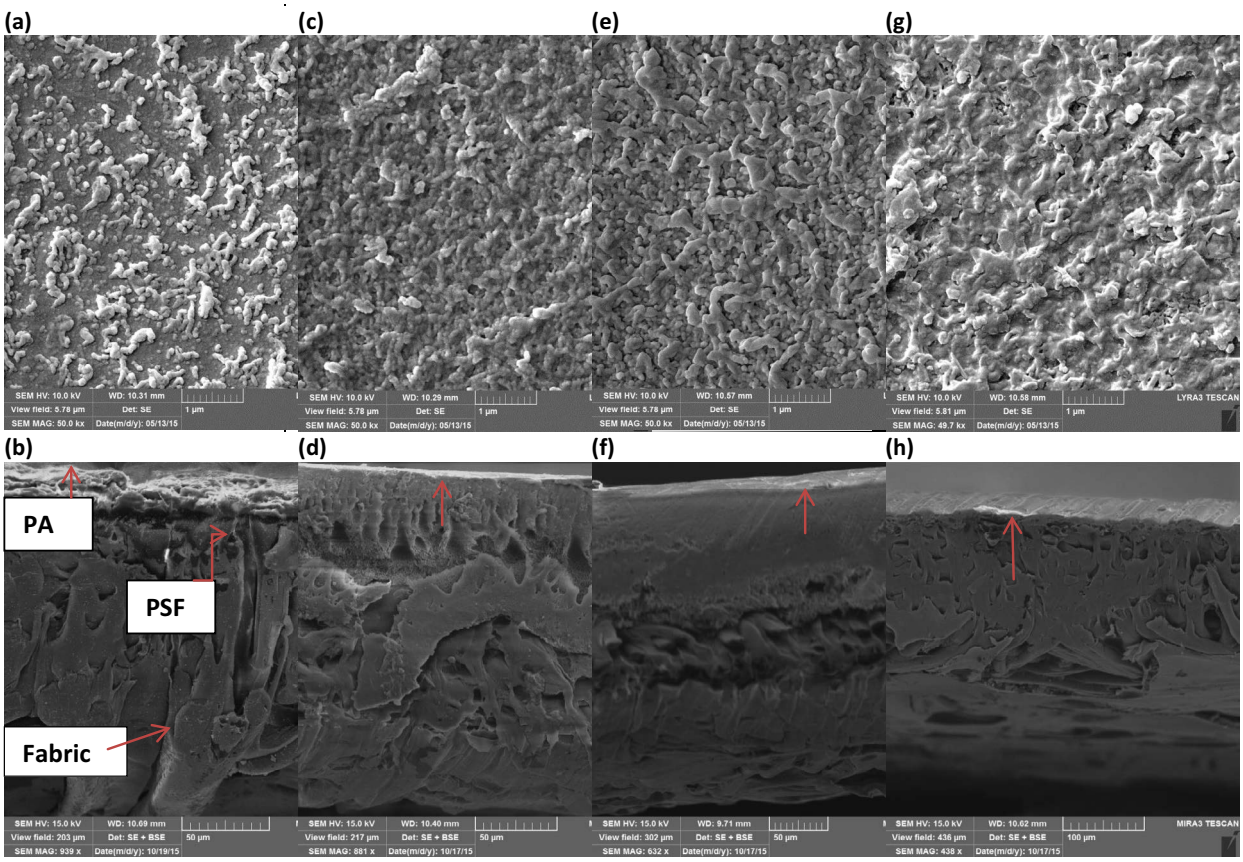

Fig. 2. Surface (a,c,e,g) and cross-section (b,d,f,h) images of the unmodified membrane (a,b) and modified membranes: 5 bilayers (c,d), 27.5 bilayers (e,f), 50 bilayers (g,h).

will contribute to increasing the resistance to water flow, and hence, it will decrease the permeate flux through membranes.

Based on the experimental results of our Box–Behnken design (Table 4), ANOVA tests were performed to identify the significant factors according to the probability *p*-value. A summary of ANOVA tests for the three responses is shown in Table 5.

The coefficient of determination for the model, R^2, is a measure of the fitting degree. A good fitting model should have a coefficient of 80% [31]. Very good models were obtained for the pure (Y_1) and saline (Y_2) permeate fluxes where the R^2 values were 0.85 and 0.86; respectively. This indicates that the models adequately represent the relationship between the studied variables. On the other hand, the salt rejection model was not as good as the other models where the R^2 value is 0.76. However, the *F*-values for the three models set off significantly from the unity which is an indication that the models are significant. Adequate precision measures the signal to noise ratio which is required to be greater than 4. The adequate precision for all models reported here indicates an adequate signal. The *p*-value (lower than 0.05) was used to determine the significant terms in Eq. (1). After removing the insignificant terms from Eq. (1), the response surface mathematical models were developed for the three responses (pure water flux (Y_1), saline water flux (Y_2), and salt rejection (Y_3)) as shown in Eqs. (8)–(10):

$$Y_1\left(\frac{\mathrm{L}}{\mathrm{m}^2\cdot\mathrm{h}}\right)=2.35X_3-1.34X_1+12.6 \tag{8}$$

$$Y_2\left(\frac{\mathrm{L}}{\mathrm{m}^2\cdot\mathrm{h}}\right)=-1.22X_1+2.36X_3-0.98X_2^2+12.10 \tag{9}$$

$$Y_3(\%)=1.87X_1+1.6X_3^2+1.67X_4^2+90.5 \tag{10}$$

Figs. 3–5 compare the predicted vs. actual values of the three measured responses. It can be observed that the model predictions were close to the actual experimental values with a little deviation of a few points. It is an indication that the developed models were productive in establishing the relationship between the studied variables and the three responses.

Residual analysis is also an effective model-validation method that was used to check the suitability of the models. The normal plot of residuals (Figs. S2–S4) showed that all residuals lie on a straight line which indicates that residuals followed a normal distribution and confirmed that there was a good correlation between the experimental data and the model prediction.

Table 3
Effect of bilayers on membrane thickness

Membrane	Thickness (nm)	R_{ms} (nm)
Pristine polyamide membrane	265	119
5 bilayers membrane	282	86
27.5 bilayers membrane	393	64
50 bilayers membrane	567	42

3.1. Interactive effects of significant factors on responses

Three-dimensional surface plots showing the mutual influence of the studied variables on permeate flux and salt rejection are depicted in Figs. 6–10. The effect of number of

Table 4
Observed responses for each experiment run

Run	Permeate flux (pure water feed)	Permeate flux (saline water feed)	Salt rejection
	Y_1, (L/m² h)	Y_2, (L/m² h)	Y_3 (%)
1	10.13	8.77	93.5
2	11.71	10.20	95.0
3	12.64	12.10	90.5
4	15.11	14.15	90.5
5	10.42	9.06	90.5
6	10.73	9.62	94.0
7	13.27	12.71	91.0
8	12.42	10.49	94.0
9	13.35	12.49	88.0
10	11.90	10.14	93.0
11	11.00	10.00	91.5
12	11.20	10.28	95.0
13	12.85	10.92	93.0
14	15.81	14.50	96.0
15	14.21	13.40	92.0
16	7.84	6.46	94.0
17	14.27	12.74	90.5
18	9.89	8.96	92.0
19	11.39	9.75	94.5
20	15.28	14.18	96.0
21	13.27	12.71	91.0
22	13.06	12.49	94.5
23	12.01	11.50	90.0
24	15.11	13.14	93.5
25	13.70	11.85	91.5
26	9.49	9.24	90.5
27	9.92	8.84	93.0
28	9.42	8.13	95.0
29	12.01	11.50	90.0

Table 5
Summary of ANOVA test for fluxes and salt rejection

Response	Y_1	Y_2	Y_3
R^2	0.85	0.86	0.76
Probability of error	0.0012	0.0007	0.0203
F-value	5.77	6.3	3.13
Probability of lack of fit	0.1063	0.1016	0.0161
Sum of squares	96.18	98.74	91.32
Mean square	6.87	7.05	6.52
Adequate precision	9.39	9.42	6.75
Significant terms	X_1, X_3	X_1, X_2, X_3	X_1, X_3^2, X_4^2

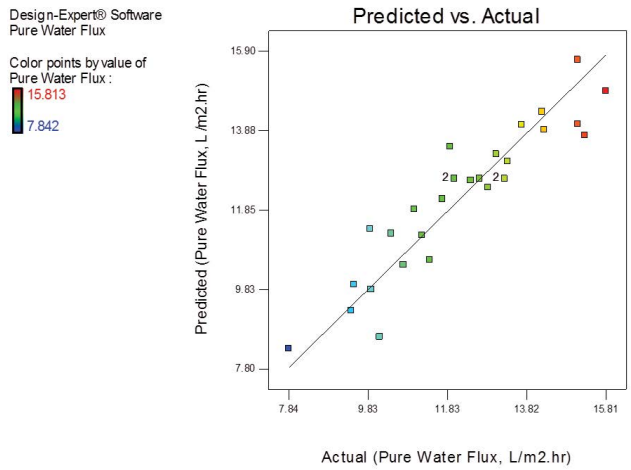

Fig. 3. Predicted vs. actual permeate flux under pure water feed.

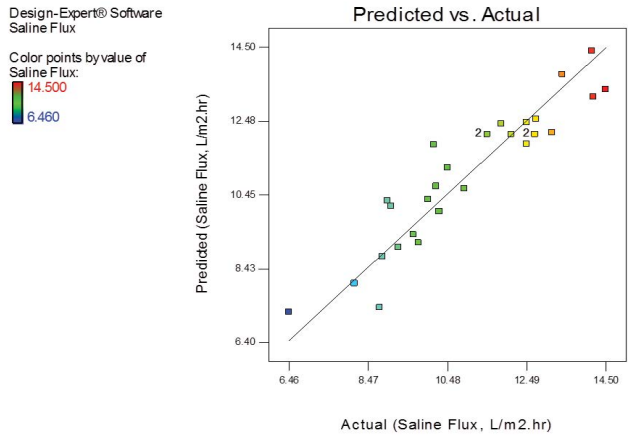

Fig. 4. Predicted vs. actual permeate flux under saline water feed.

layers and PEI concentration on pure water flux at a fixed concentration of PAH (110 mg/L) and a fixed pH of 6.0 is shown in Fig. 6. It was observed that the pure water flux is directly proportional to the PEI concentration and decreases with the number of coated layers. Higher PEI concentration has a strong effect on pure water flux since it will enhance the hydrophilic functional groups on the membrane surface that will promote water flow. By increasing the PEI concentration from 20 to 200 mg/L, pure water flux was increased from 10.42 to 15.11 L/m^2 h, which is an increase of more than 31%. This indicates that PEI concentration has a stronger effect on the water flux than that of the number of bilayers. On the other hand, the pure water flux of the unmodified polyamide membrane was 16 L/m^2 h which is slightly higher than that of the modified membranes. The decrease in permeate flux of the modified membrane is the result of additional thickness on the polyamide membrane surface that increases the resistance for mass transfer and hence, the permeate flux.

Fig. 7 shows the effect of the number of layers and PEI concentration on saline water flux at a fixed pH of 6 and a

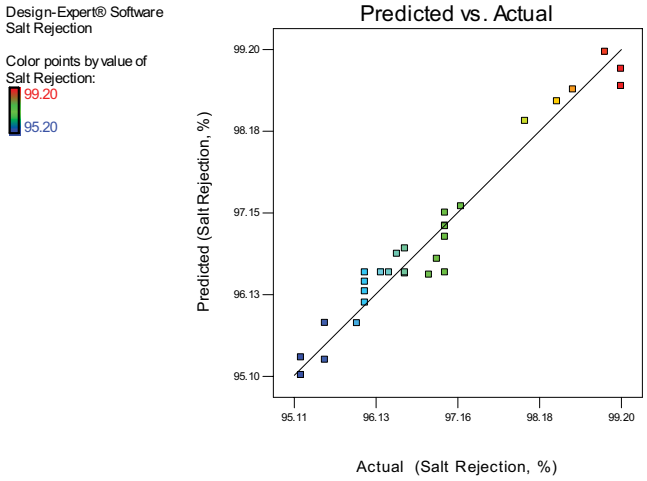

Fig. 5. Predicted vs. actual salt rejection.

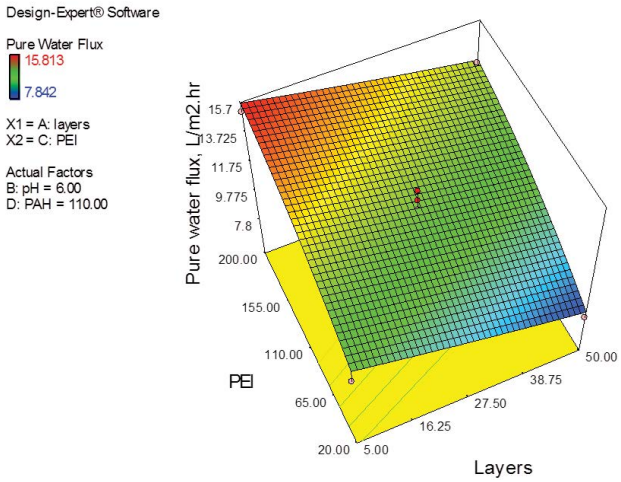

Fig. 6. Response plot of pure water flux (Y_1) vs. the number of layers and PEI concentration (pH = 6; PAH = 110 mg/L).

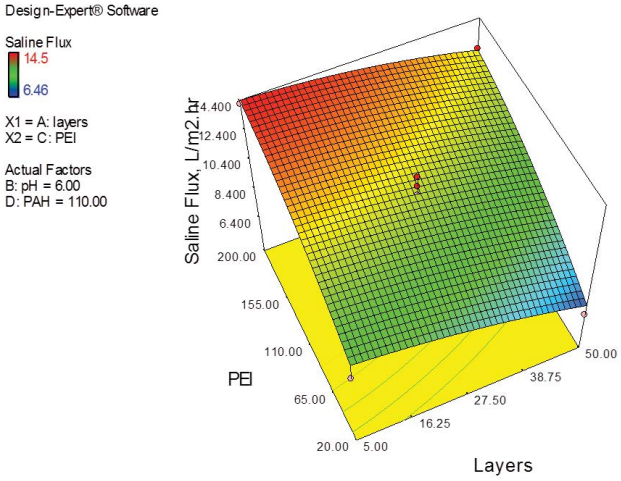

Fig. 7. Response plot of saline flux (Y_2) vs. the number of layers and PEI concentration (pH = 6; PAH = 110 mg/L).

concentration of 110 mg/L PAH. It can be seen that a lower number of layers and high PEI concentrations are in favor of higher permeation flux. With 5 layers and PEI concentration of 200 mg/L, the permeate flux was at the maximum of 14.15 L/m^2 h. This can be explained in terms of increasing smoothness and hydrophilicity by depositing higher PEI concentration. Unmodified polyamide membrane showed apermeate flux of 8.1 L/m^2 h which proved that our polyelectrolytes successfully enhanced the membrane performance in saline conditions.

A similar trend was observed when the effect of pH and PEI concentration on saline flux (Y_2) was studied as shown in Fig. 9. It can be seen that under saline conditions, higher pH and higher PEI concentration, favors higher permeate flux.

Fig. 9 shows the effect of concentration of both polyelectrolytes on salt rejection while keeping the pH and number of layers constant. It shows some interesting behavior that is different from the previous results. A similar concentration of both polyelectrolytes favors salt rejection. A more compact and dense structure is likely obtained at these concentrations that have increased the salt rejection. For example, at 20 mg/L, the salt rejection was 95% but when the concentration increased to 200 mg/L for both polyelectrolytes, the salt rejection increased to 96%. However, PEI has a dominant impact on salt rejection. The salt rejection was 90.5% with 20 mg/L PEI but escalated to 96% by increasing the PEI to 200 mg/L (keeping the second polyelectrolyte at a constant concentration of 200 mg/L in both conditions). The macromolecules in dilute polyelectrolyte solutions are well stretched and dispersed, and the membrane binding-sites are sufficient for the chains of PEI/PAH polyelectrolytes. Therefore, a relatively loose skin selective layer is formed on the membrane surface. However, as the polyelectrolyte concentration increases, polyelectrolyte-stretching decreases due to the charge balance of the counter-ion. Besides, more hydrophilic functional groups will be present on the surface that will increase the water adsorption and flux. Nonetheless, a further increase in polyelectrolyte concentrations above a "critical concentration" will result in entanglement and aggregation of the macromolecules that will lead to a dense and thicker layer with lower permeation flux. In our experiment, it looks that we did not reach this critical concentration while other researchers reported it around 1,000 mg/L [32].

Fig. 10 shows the contour plot of salt rejection vs. the number of layers and PAH concentration. It can be seen that an increase in the layer number has a profound effect on salt rejection compared to an increase of PAH concentration. Around 90% salt rejection was achieved by depositing five bilayers of polyelectrolytes at 20 mg/L PAH. However, there was only a 1% increase in salt rejection by increasing the PAH concentration up to 10 times. On the other hand, salt rejection increased to 95% by depositing 50 bilayers of polyelectrolytes due to an increase in thickness of the dense structure.

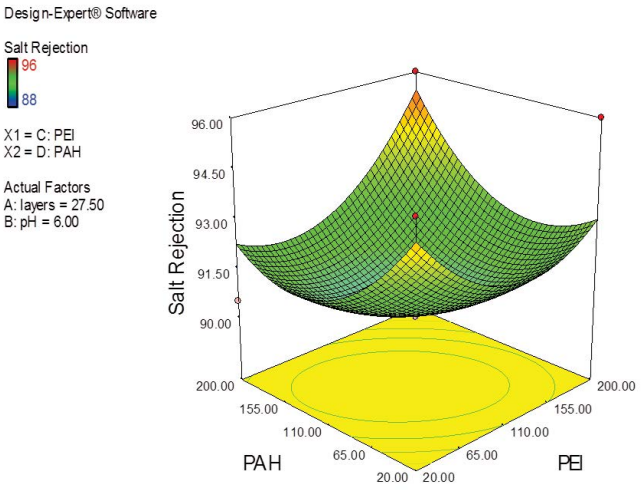

Fig. 9. Response plot of salt rejection (Y_3) vs. PAH and PEI concentrations (layers = 27.5; pH = 6).

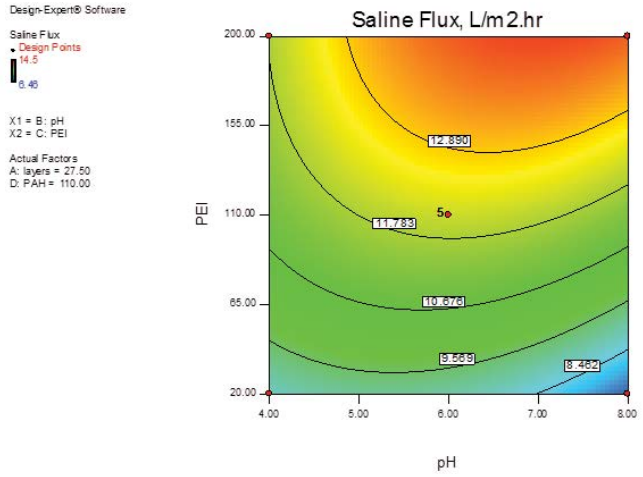

Fig. 8. Response plot of saline flux (Y_2) vs. the pH and PEI concentration (layers = 27.5; PAH = 110 mg/L).

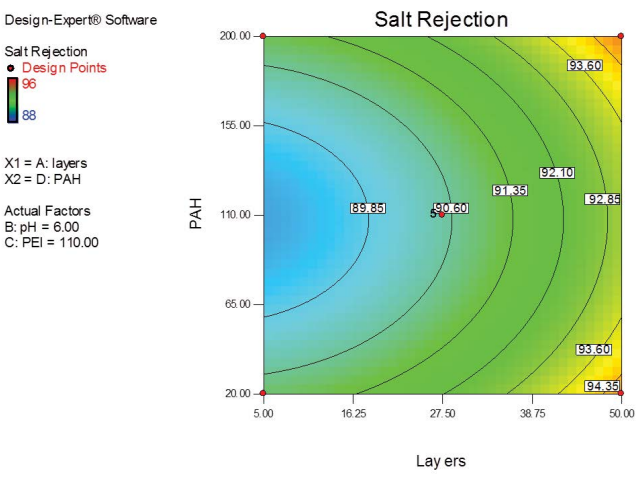

Fig. 10. Contour plot of salt rejection (Y_3) vs. the number of layers and PAH concentration (pH = 6; PAH = 110 mg/L).

Table 6
Optimum level predictions compared with the performance of the unmodified membrane

Constraint	Optimum level	Unmodified membrane
Number of layers	50	–
pH	7.8	–
PEI, (mg/L)	200	–
PAH, (mg/L)	200	–
Pure water flux, (L/m^2 h)	14.64	16.0
Saline flux, (L/m^2 h)	12.85	8.1
Salt rejection, (%)	99	95

Table 7
Comparison of the experimental and predicted responses of the optimum membrane

Response	Experimental	Predicted	Error (%)
Pure water flux, (L/m^2 h)	12.28	14.64	16.12
Saline flux, (L/m^2 h)	11.56	12.85	10.04
Salt rejection, (%)	97	99	2.02

4. Response surface optimization

To optimize the membrane preparation conditions, desired goals were set and all the input variables were taken within the range while all the responses were set to the maximum level. Inputs were set at a significance of 3 which shows a medium satisfactory level. All responses were set at high importance of 5 and the optimization was run for 30 cycles. All of these constraints are given in Table S4. The overall desirability of the optimized solution was 0.873 (a value close to unity is considered as good). The optimum conditions of the independent variables and the predicted responses are summarized in Table 6. It was revealed that both polyelectrolytes must be used at their maximum concentration at a pH of 7.8 with 50 bilayers of polyelectrolyte coating. By comparing the optimum membrane with the unmodified membrane, it can be seen that although some of the pure water flux was lost by adding polyelectrolyte layers on the membrane surface, the compensation was achieved in terms of higher saline flux and better salt rejection.

4.1. Confirmation run

Confirmation run was done by considering the optimized conditions (50 layers were deposited at a pH of 7.8, and a concentration of 200 mg/L of PEI/PAH). Experimental values after the confirmation run and the predicted values through response surface optimization along with the error are shown in Table 7. Roughly speaking, a good agreement was achieved between the prediction and the experimental observations. However, the most important thing is that we were able to optimize the preparation conditions such that all three responses were maximized.

5. Conclusions

RSM was applied in this work to find the significant parameters of the LbL assembly of polyelectrolytes for tuning the properties of the modified membranes. The most influential parameters on the salt rejection property of the membrane were the number of layers and the concentration of both polyelectrolytes. ANOVA study showed that the developed models have adequately represented the relationship between the studied variables and the responses. Optimization showed that both the polyelectrolytes must be used at their maximum concentration with a pH of 7.8 to modify the existing polyamide layer with 50 bilayers. The confirmation run revealed that actual values are comparable to the predicted ones with an acceptable margin of error. The predictive models will help to tune the membrane modification recipe.

Acknowledgment

The authors would like to gratefully acknowledge the financial support from King Fahd University of Petroleum and Minerals (KFUPM) grant number DISC1503.

Symbols

A	—	Number of layers
A	—	Active membrane area, m^2
b	—	Polynomial coefficient
C	—	Polyethylenemine concentration, mg/L
C_p	—	Feed salt concentration, mg/L
C_f	—	Concentrations of salt in the permeate, mg/L
D	—	Poly(allylamine hydrochloride) concentration, mg/L
J_0	—	Volumetric flux, L/m^2 h
R_{NaCl}	—	Salt rejection, %
t	—	Permeation time, h
V	—	Permeate volume, L
X	—	Coded independent variable
Y	—	Predicted response

References

[1] L.F. Greenlee, D.F. Lawler, B.D. Freeman, B. Marrot, P. Moulin, Reverse osmosis desalination: Water sources, technology, and today's challenges, Water Res., 43 (2009) 2317–2348.

[2] WHO, UNICEF, Progress on Drinking Water and Sanitation, World Health Organization, United Nations Children's Fund (UNICEF), UNICEF, New York and WHO, Geneva, 2008, p. 58.

[3] M.A. Montgomery, M. Elimelech, Water and sanitation in developing countries: including health in the equation, Environ. Sci. Technol., 41 (2007) 17–24.

[4] K.P. Lee, T.C. Arnot, D. Mattia, A review of reverse osmosis membrane materials for desalination—development to date and future potential, J. Membr. Sci., 370 (2011) 1–22.

[5] M.A. Shannon, P.W. Bohn, M. Elimelech, J.G. Georgiadis, B.J. Mariñas, A.M. Mayes, Science and technology for water purification in the coming decades, Nature, 452 (2008) 301–310.

[6] N. Ghaffour, T.M. Missimer, G.L. Amy, Technical review and evaluation of the economics of water desalination: current and future challenges for better water supply sustainability, Desalination, 309 (2013) 197–207.

[7] S. Burn, M. Hoang, D. Zarzo, F. Olewniak, E. Campos, B. Bolto, O. Barron, Desalination techniques — a review of the opportunities for desalination in agriculture, Desalination, 364 (2015) 2–16.

[8] RO membranes and components market is growing at 10.5% CAGR, Membr. Technol., 2015 (2015) 4, https://doi.org/10.1016/S0958-2118(15)30092-6.

[9] BCC Research, Major Reverse Osmosis System Components for Water Treatment: The Global Market, Dubin, 2020. Available at: ResearchAndMarkets.com

[10] S.A. Avlonitis, K. Kouroumbas, N. Vlachakis, Energy consumption and membrane replacement cost for seawater RO desalination plants, Desalination, 157 (2003) 151–158.

[11] R. Malaisamy, A. Talla-Nwafo, K.L. Jones, Polyelectrolyte modification of nanofiltration membrane for selective removal of monovalent anions, Sep. Purif. Technol., 77 (2011) 367–374.

[12] J.W. Park, J.Y. Park, S.H. Kim, J.H. Cho, J. Bang, Desalination membranes from pH-controlled and thermally-crosslinked layer-by-layer assembled multilayers, J. Mater. Chem., 20 (2010) 2085–2091.

[13] C.L. Wang, G.K. Such, A. Widjaya, H. Lomas, G. Stevens, F. Caruso, S.E. Kentish, Click poly(ethylene glycol) multilayers on RO membranes: fouling reduction and membrane characterization, J. Membr. Sci., 409–410 (2012) 9–15.

[14] T. Ishigami, K. Amano, A. Fujii, Y. Ohmukai, E. Kamio, T. Maruyama, H. Matsuyama, Fouling reduction of reverse osmosis membrane by surface modification via layer-by-layer assembly, Sep. Purif. Technol., 99 (2012) 1–7.

[15] J. Saqib, I.H. Aljundi, Membrane fouling and modification using surface treatment and layer-by-layer assembly of polyelectrolytes: state-of-the-art review, J. Water Process Eng., 11 (2016) 68–87.

[16] I.H. Aljundi, Bromate formation during ozonation of drinking water: a response surface methodology study, Desalination, 277 (2011) 24–28.

[17] G.W. Oehlert, A First Course in Design and Analysis of Experiments, University of Minnesota, 2003.

[18] J. Sacks, W.J. Welch, T.J. Mitchell, H.P. Wynn, J. Welch, Design and analysis of computer experiments, Inst. Math. Stat., 4 (2014) 409–423.

[19] M. Khayet, C. Cojocaru, M. Essalhi, Artificial neural network modeling and response surface methodology of desalination by reverse osmosis, J. Membr. Sci., 368 (2011) 202–214.

[20] N.F. Razali, A.W. Mohammad, N. Hilal, C.P. Leo, J. Alam, Optimisation of polyethersulfone/polyaniline blended membranes using response surface methodology approach, Desalination, 311 (2013) 182–191.

[21] S. Javed, I.H. Aljundi, M. Khaled, High fouling-resistance of polyamide desalination-membrane modified with PEI/PAH polyelectrolyte multilayers, J. Environ. Chem. Eng., 5 (2017) 4594–4604.

[22] J.T. Duan, Y.C. Pan, F. Pacheco, E. Litwiller, Z.P. Lai, I. Pinnau, High-performance polyamide thin-film-nanocomposite reverse osmosis membranes containing hydrophobic zeolitic imidazolate framework-8, J. Membr. Sci., 476 (2015) 303–310.

[23] Y.-N. Kwon, S.P. Hong, H.W. Choi, T. Tak, Surface modification of a polyamide reverse osmosis membrane for chlorine resistance improvement, J. Membr. Sci., 415–416 (2012) 192–198.

[24] J.-E. Gu, S. Lee, C.M. Stafford, J.S. Lee, W. Choi, B.-Y. Kim, K.-Y. Baek, E.P. Chan, J.Y. Chung, J. Bang, J.-H. Lee, Molecular layer-by-layer assembled thin-film composite membranes for water desalination, Adv. Mater., 25 (2013) 4778–4782.

[25] H. Tanaka, L. Ödberg, L. Wågberg, T. Lindström, Exchange of cationic polyacrylamides adsorbed on monodisperse polystyrene latex and cellulose fibers: effect of molecular weight, J. Colloid Interface Sci., 134 (1990) 229–234.

[26] R. Ramachandran, P. Somasundaran, Competitive adsorption of polyelectrolytes: a size exclusion chromatographic study, J. Colloid Interface Sci., 120 (1987) 184–188.

[27] L.Y. Ng, A.W. Mohammad, C.Y. Ng, C.P. Leo, R. Rohani, Development of nanofiltration membrane with high salt selectivity and performance stability using polyelectrolyte multilayers, Desalination, 351 (2014) 19–26.

[28] B.-H. Jeong, E.M.V. Hoek, Y. Yan, A. Subramani, X.F. Huang, G. Hurwitz, A.K. Ghosh, A. Jawor, Interfacial polymerization of thin film nanocomposites: a new concept for reverse osmosis membranes, J. Membr. Sci., 294 (2007) 1–7.

[29] F.A. Pacheco, I. Pinnau, M. Reinhard, J.O. Leckie, Characterization of isolated polyamide thin films of RO and NF membranes using novel TEM techniques, J. Membr. Sci., 358 (2010) 51–59.

[30] J.H. Seo, J.L. Lutkenhaus, J. Kim, P.T. Hammond, K. Char, Effect of the layer-by-layer (LbL) deposition method on the surface morphology and wetting behavior of hydrophobically modified PEO and PAA LbL films, Langmuir, 24 (2008) 7995–8000.

[31] P.P. Qiu, M.C. Cui, K.L. Kang, B. Park, Y.Y. Son, E.Y. Khim, M. Jang, J.Y. Khim, Application of Box–Behnken design with response surface methodology for modeling and optimizing ultrasonic oxidation of arsenite with H_2O_2, 12 (2014) 164–172.

[32] J. Xu, X.S. Feng, C.J. Gao, Surface modification of thin-film-composite polyamide membranes for improved reverse osmosis performance, J. Membr. Sci., 370 (2011) 116–123.

Supplementary information

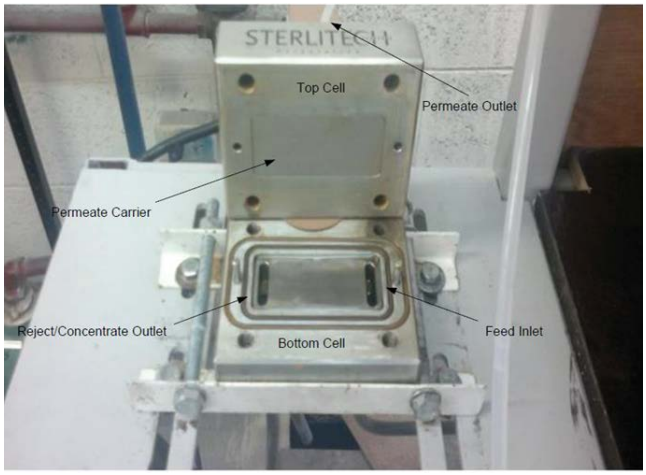

Fig. S1. Membrane assembly CF-042.

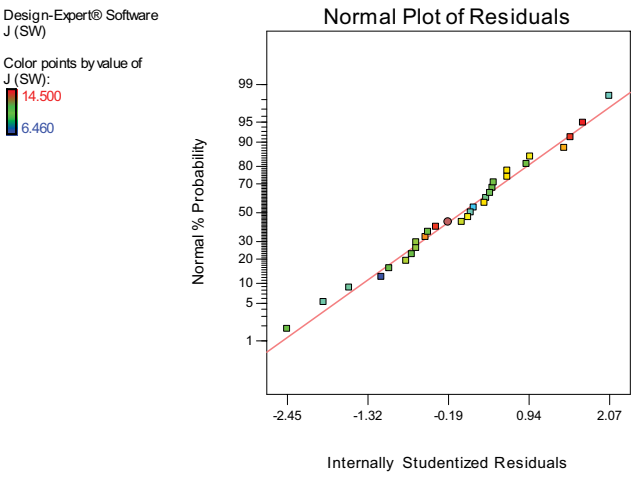

Fig. S2. The normal plot of residuals for response Y_1.

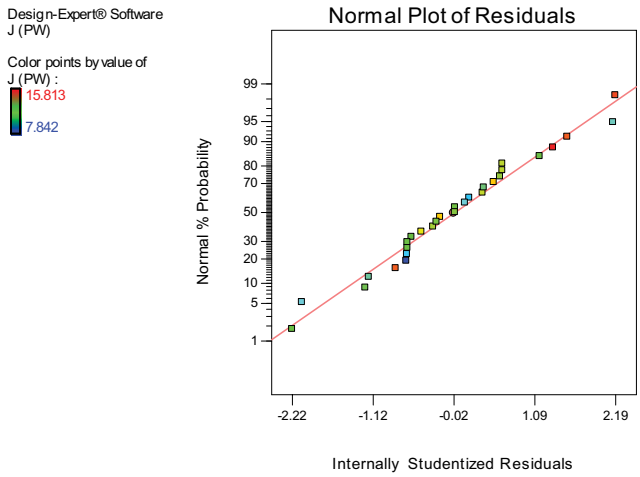

Fig. S3. The normal plot of residuals for response Y_2.

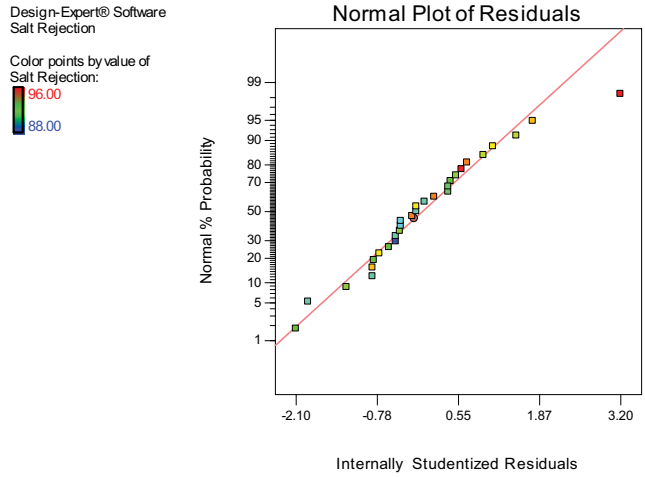

Fig. S4. The normal plot of residuals for response Y_3.

Table S1
Response Y_1, permeate flux with pure water feed

ANOVA for response surface quadratic model					
Analysis of variance table (partial sum of squares – type III)					
Source	Sum of squares	DF	Mean square	*F*-value	*p*-value Prob. > *F*
Model	96.18	14	6.87	5.77	0.0012
X_1	21.4	1	21.4	17.98	0.0008
X_2	0.077	1	0.077	0.065	0.8025
X_3	66.08	1	66.08	55.52	0.0001
X_4	2.42	1	2.42	2.04	0.1755
X_1X_2	0.61	1	0.61	0.52	0.4842
X_1X_3	0.07	1	0.07	0.059	0.8117
X_1X_4	0.6	1	0.6	0.51	0.4885
X_2X_3	1.1	1	1.1	0.93	0.3524
X_2X_4	0.12	1	0.12	0.098	0.7593
X_3X_4	0.052	1	0.052	0.044	0.8372
X_1^2	0.034	1	0.034	0.029	0.8677
X_2^2	1.56	1	1.56	1.31	0.2719
X_3^2	2.25	1	2.25	1.89	0.191
X_4^2	0.054	1	0.054	0.045	0.8342
Residual	16.66	14	1.19		
Lack of fit	15.06	10	1.51	3.77	0.1063
Pure error	1.597696	4	0.399424		

Table S2
Response Y_2, permeate flux with saline water feed

ANOVA for response surface Quadratic model					
Analysis of variance table (partial sum of squares – type III)					
Source	Sum of squares	DF	Mean square	*F*-value	*p*-value Prob. > *F*
Model	98.74115	14	7.052939	6.301014419	0.0007
X_1	17.83641	1	17.83641	15.93484114	0.0013
X_2	0.213333	1	0.213333	0.190589535	0.6691
X_3	67.02413	1	67.02413	59.87858638	0.0001
X_4	1.062075	1	1.062075	0.948845535	0.3465
X_1X_2	0.3481	1	0.3481	0.310988518	0.5859
X_1X_3	0.2209	1	0.2209	0.197349508	0.6637
X_1X_4	0.540225	1	0.540225	0.482630774	0.4986
X_2X_3	2.772225	1	2.772225	2.476673787	0.1379
X_2X_4	0.093025	1	0.093025	0.08310746	0.7774
X_3X_4	0.156025	1	0.156025	0.139390932	0.7145
X_1^2	0.777659	1	0.777659	0.694751373	0.4185
X_2^2	6.197878	1	6.197878	5.537112938	0.0338
X_3^2	3.223946	1	3.223946	2.880236062	0.1118
X_4^2	1.762389	1	1.762389	1.574497537	0.2301
Residual	15.67068	14	1.119334		
Lack of fit	14.20658	10	1.420658	3.881312752	0.1016
Pure error	1.4641	4	0.366025		

Table S3
Response Y_3, salt rejection

ANOVA for response surface quadratic model					
Analysis of variance table (partial sum of squares – type III)					
Source	Sum of squares	DF	Mean square	*F*-value	*p*-value Prob. > *F*
Model	91.31968	14	6.522835	3.133199	0.0203
X_1	42.1875	1	42.1875	20.26447	0.0005
X_2	1.333333	1	1.333333	0.640457	0.4369
X_3	2.520833	1	2.520833	1.210865	0.2897
X_4	0.083333	1	0.083333	0.040029	0.8443
X_1X_2	9	1	9	4.323088	0.0565
X_1X_3	0.0625	1	0.0625	0.030021	0.8649
X_1X_4	0	1	0	0	1.0000
X_2X_3	0.5625	1	0.5625	0.270193	0.6113
X_2X_4	0.0625	1	0.0625	0.030021	0.8649
X_3X_4	5.0625	1	5.0625	2.431737	0.1412
X_1^2	3.448761	1	3.448761	1.656589	0.2189
X_2^2	5.45045	1	5.45045	2.618086	0.1280
X_3^2	16.692	1	16.692	8.017889	0.0133
X_4^2	18.01802	1	18.01802	8.654831	0.0107
Residual	29.14583	14	2.081845		
Lack of fit	28.14583	10	2.814583	11.25833	0.0161
Pure error	1	4	0.25		

Table S4
Optimization constraints

Name	Goal	Lower limit	Upper limit	Upper importance
Layers	in range	5	50	3
pH	in range	4	8	3
PEI	in range	20	200	3
PAH	in range	20	200	3
Pure flux	maximize	7.84	15.81	5
Saline flux	maximize	6.46	14.5	5
Salt rejection	maximize	88	99.99	5